Globo H Is a Promising Theranostic Marker for Intrahepatic Cholangiocarcinoma

Tsai-Hsien Hung,[1*] Jung-Tung Hung,[1*] Chiao-En Wu,[2*] Yenlin Huang,[3,9] Chien-Wei Lee,[1] Chau-Ting Yeh,[4] Yi-Hsiu Chung,[5] Fei-Yun Lo,[1] Li-Chun Lai,[1] John K. Tung,[1] John Yu,[1,7,9] Chun-Nan Yeh,[6] and Alice L. Yu[1,8,9]

Recent studies support the development of cancer therapeutics to target Globo H-ceramide, the most prevalent tumor-associated carbohydrate antigen in epithelial cancers. Herein, we evaluated the expression of Globo H and its prognostic significance in intrahepatic cholangiocarcinoma (ICC) and conducted preclinical studies to assess the antitumor activity of Globo H–specific antibody in thioacetamide (TAA)–induced ICC in rats. Globo H–ceramide in tumor specimens was detected by immunohistochemistry (IHC) and mass spectrometry. Antitumor efficacy of anti–Globo H mAbVK9 was evaluated in TAA-induced ICC in rat. Natural killer (NK) cells and their related genes were analyzed by IHC and quantitative real-time polymerase chain reaction. Data mining revealed that B3GALT5 and FUT2, the key enzymes for Globo H biosynthesis, were significantly up-regulated in human ICC. In addition, Globo H expression was detected in 41% (63 of 155) of ICC tumor specimens by IHC staining, and validated by mass spectrometric analysis of two IHC-positive tumors. Patients with Globo H positive tumors had significantly shorter relapse-free survival (RFS) and overall survival (P = 0.0003 and P = 0.002, respectively). Multivariable Cox regression analysis identified Globo H expression as an independent unfavorable predictor for RFS (hazard ratio: 1.66, 95% confidence interval: 1.08-2.36, P = 0.02) in ICC. Furthermore, gradual emergence of Globo H in liver tissues over 6 months in TAA-treated rats recapitulated the multistage progression of ICC *in vivo*. Importantly, administration of anti-Globo H mAbVK9 in rats bearing TAA-induced ICC significantly suppressed tumor growth with increased NK cells in the tumor microenvironment. *Conclusion:* Globo H is a theranostic marker in ICC. (*Hepatology Communications* 2022;6:194-208).

Cholangiocarcinoma (CCA) is a malignant tumor of biliary epithelial origin and is the second-most common primary liver cancer after hepatocellular carcinoma (HCC). Over the last three decades, incidence and mortality of CCA, especially intrahepatic cholangiocarcinoma (ICC), have been rising worldwide, with higher rates found in Asian countries due to a combination of genetic and geographic determinants that increase the prevalence of risk factors such as hepatolithiasis, liver fluke infection, and viral hepatitis.[1] Currently, surgical resection and chemotherapy remain to be the only major therapeutic modalities. Unfortunately, due to the insidious and aggressive nature of ICC, diagnosis is usually made at an advanced stage, leading to high morbidity and poor outcome.[2] Even among

Abbreviations: ^{18}*F-FDG-PET, 2-deoxy-2-[F-18]-fluoro-D-glucose positron emission tomography; ADCC, antibody-dependent cell-mediated cytotoxicity; B3GALT5, beta-1,3-galactosyltransferase 5; BTC, biliary tract cancer; CCA, cholangiocarcinoma; CDC, complement-dependent cytotoxicity; cDNA, complementary DNA; CI, confidence interval; FGFR, fibroblast growth factor receptor; FUT1, fucosyltransferase 1; FUT2, fucosyltransferase 2; GHCer, Globo H ceramide; GSL, glycosphingolipid; HR, hazard ratio; ICC, intrahepatic cholangiocarcinoma; IDH1, isocitrate dehydrogenase 1; IHC, immunohistochemical; IL, interleukin; MALDI-TOF, matrix-assisted laser desorption ionization–time of flight; NK, natural killer cell; NTRK, neurotrophic receptor tyrosine kinase; OS, overall survival; PBS, phosphate-buffered saline; PCR, polymerase chain reaction; RFS, relapse-free survival; SUV, standardized uptake value; TAA, thioacetamide; TIGER-LC, Thailand Initiative in Genomics and Expression Research for Liver Cancer; T/L, tumor-to-liver ratio.*

Received May 3, 2021; accepted July 14, 2021.

Additional Supporting Information may be found at onlinelibrary.wiley.com/doi/10.1002/hep4.1800/suppinfo.

Supported by Chang Gung Medical Foundation (OMRPG3C0017, OMRPG3C0018, OMRPG3C0047, and OMRPG3C0048); Ministry of Science and Technology, Taiwan (MOST 107-2314-B-182A-134-MY3, MOST 109-2314-B-182-080-MY3, and MOST 109-2321-B-182A-005); and Chang Gung Memorial Hospital, Linkou (CMRPG3J0311, CMRPG3J0312, CMRPG3J0971, CMRPG3J0972, CMRPG3J0973, and CMRPG3K0711).

those who undergo tumor resection, clinical outcomes have been disappointing. In a systematic review of 42 index studies containing 4,756 patients with ICC who received curative-intent surgery, 5-year overall survival (OS) rarely exceeded 30%-35%, and only 2%-39% of patients were recurrence-free at 5 years.[3] These sobering statistics emphasize the need to identify additional biomarkers that can not only help predict clinical outcome but also serve as therapeutic targets.

Advances in sequencing technology and increasing accessibility to tumor profiling in recent years have led to the identification of several potential biomarkers for ICC, including *KRAS* (proto-oncogene GTPase), *PIK3CA* (phosphatidylinositol-4,5-bisphosphate 3-kinase catalytic subunit α), *TP53* (tumor protein p53), isocitrate dehydrogenase 1 (*IDH1*), fibroblast growth factor receptor 2 (*FGFR2*), neurotrophic receptor tyrosine kinase (*NTRK*), and *ERBB2* (Erb-B2 receptor tyrosine kinase 2), as putative targets for personalized therapy.[4] In particular, two targeted agents, larotrectinib and pemigatinib, have been approved by the Food and Drug Administration for patients with cancers containing NTRK and FGFR2 fusion genes, respectively.[5] However, *FGFR2* rearrangements occur in less than 20% of ICC cases,[6] and only 1 of 28 samples harbors the *RABGAP1L-NTRK1* gene fusion,[7] making *FGFR2* and *NTRK* inhibitors clinically relevant only for a relatively small subset of patients. In addition, ivosidenib, a small-molecule inhibitor of mutated IDH1, improved progression-free survival of patients with ICC with *IDH1* mutations; however, the IDH1 mutation was found in only approximately 13% of patients with ICC.[8] Consequently, characterizing additional actionable molecular targets is needed to provide opportunities for developing therapeutics.

The approval of dinutuximab, an anti-GD2 (disialoganglioside) antibody for the treatment of neuroblastoma,[9] has piqued the interest in targeting tumor-associated carbohydrate antigens in recent years. Glycomic profiling of tumor tissues has consistently shown alterations in the N-glycosylation and O-glycosylation profiles of surface glycoproteins and glycosphingolipids, which contribute to cancer proliferation, invasion, angiogenesis, and metastasis.[10,11]

*These authors contributed equally to this work.

View this article online at wileyonlinelibrary.com.
DOI 10.1002/hep4.1800

Potential conflict of interest: Nothing to report.

ARTICLE INFORMATION:

From the [1]Institute of Stem Cell and Translational Cancer Research, Chang Gung Memorial Hospital at Linkou, Taoyuan, Taiwan; [2]Department of Hematology-Oncology, Chang Gung Memorial Hospital, Chang Gung University, Taoyuan, Taiwan; [3]Department of Anatomic Pathology, Chang Gung Memorial Hospital at Linkou, Taoyuan, Taiwan; [4]Liver Research Center, Department of Hepato-Gastroenterology, Chang Gung Memorial Hospital and College of Medicine, Chang Gung University, Taoyuan, Taiwan; [5]Department of Medical Research and Development, Chang Gung Memorial Hospital, Taoyuan, Taiwan; [6]Department of Surgery and Liver Research Center, Chang Gung Memorial Hospital, Chang Gung University, Taoyuan, Taiwan; [7]Institute of Cellular and Organismic Biology, Academia Sinica, Taipei, Taiwan; [8]Department of Pediatrics, University of California in San Diego, San Diego, CA; [9]Chang Gung University, Taoyuan, Taiwan.

ADDRESS CORRESPONDENCE AND REPRINT REQUESTS TO:

Chun-Nan Yeh, M.D.
Department of Surgery and Liver Research Center
Chang Gung Memorial Hospital, Chang Gung University
No. 5, Fuxing Street
Guishan District, Taoyuan City 333, Taiwan
E-mail: yehchunnan@gmail.com
Tel.: +1-886-328-1200
or

Alice L. Yu, M.D., Ph.D.
Institute of Stem Cell and Translational Cancer Research
Chang Gung Memorial Hospital at Linkou
No. 15, Wen-Hua 1st Road
Guishan District, Taoyuan City 333, Taiwan
E-mail: a1yu@health.ucsd.edu
Tel.: +1-886-328-1200

These changes have also been reported in CCA cells lines, patient sera, and tumor tissues, such as aberrant O-linked glycosylation on mucin 1, increased expression of high-mannose glycans, sWGA-specific glycans, SJA-specific N-acetylgalactosamine-associated glycans, hexosylceramides, and lactosylceramides, leading to investigations of their clinical utility as diagnostic and prognostic biomarkers.[12] However, the expression of Globo H ceramide (GHCer), the most prevalent tumor-associated glycan, has not been explored in ICC. Globo H is overexpressed on the surface of many common cancers, including those of the breast, lung, stomach, and pancreas.[13,14] Our group has demonstrated that GHCer promotes tumor angiogenesis and escape from immune surveillance, providing the rationales for developing Globo H–targeted immunotherapy.[15,16] A multinational phase 2 randomized controlled trial of a Globo H vaccine in metastatic breast cancer has shown encouraging results with a low toxicity profile and significant survival benefit for patients who generate effective humoral responses against Globo H.[13] Whether Globo H has theranostic potential for ICC has yet to be investigated.

In this study, we showed that Globo H is expressed in ICC, as in most other epithelial cancers, and its expression correlated with inferior patient survival. We also demonstrated preclinical efficacy of Globo H–targeted therapy for ICC using a monoclonal antibody against Globo H, in a rat model of thioacetamide (TAA)–induced ICC. Our data point to a new direction for the treatment of ICC by targeting Globo H.

Patients and Methods

CLINICAL SAMPLES AND ARRAY DATA

Formalin-fixed, paraffin-embedded (FFPE) tumor tissue specimens from 155 patients with American Joint Committee on Cancer stages I to III ICC as well as their relevant clinical and pathological data and snap-frozen ICC tissues used for glycosphingolipid (GSL) extraction were obtained from Linkou Chang Gung Memorial Hospital, Taoyuan, Taiwan. Written, informed consent was obtained from all subjects before their tissues were deposited. All protocols were carried out in accordance with relevant guidelines and regulations and approved by the institutional review board of the Chang Gung Medical Foundation (reference number 201304768B0 and 201700831A3C502). Thailand Initiative in Genomics and Expression Research for Liver Cancer (TIGER-LC) data were downloaded from NCBI's Gene Expression Omnibus (accession number GSE76311), and all expression data were log2-transformed for analyses.

TAA-INDUCED ICC IN RATS

The Experimental Animal Ethics Committee of Chang Gung Memorial Hospital approved all animal protocols used in this study (Institutional Animal Care and Use Committee number 2018092502). The adult male Sprague–Dawley rats (weight = 319 ± 14 g, mean ± SD) used in these experiments were housed in specific-pathogen-free condition. Food and water were available *ad libitum*, with 300 mg/L of TAA administered daily to their drinking water.[17] At 24 weeks, the rats were randomly divided into a control group (n = 4) and treatment group (n = 5) that received weekly intravenous injections of phosphate-buffered saline (PBS; pH 7.4) or Globo H antibody (VK9) (300 μg), respectively, over a 2-month period. During the course of treatment, the animals were weighed every week to monitor changes in body weight.

EVALUATION OF TREATMENT EFFICACY IN RATS BY POSITRON EMISSION TOMOGRAPHY

To monitor ICC tumors in rat liver, 2-deoxy-2-[F-18]-fluoro-D-glucose positron emission tomography (^{18}F-FDG-PET) scans were performed at the Molecular Imaging Center of Linkou Chang Gung Memorial Hospital. At week 24, TAA-treated rats that showed ^{18}F-FDG-PET-detectable ICC were subjected to serial PET scanning at 4-week intervals using the nanoScan PET/computed tomography imaging system (Mediso, Hungary).[18] Details regarding the preparation of radioligands, acquisition of emission data, and determination of optimal scanning duration have been previously reported.[19] Detailed methods are described in the Supporting Information.

IMMUNOHISTOCHEMISTRY

The primary antibodies used included VK9, a monoclonal antibody against Globo H (hybridoma

generously provided by Dr. Govindaswami Ragupathi (Memorial Sloan-Kettering Cancer Center, New York, NY) and anti-Ki-67 (NCL-L-Ki67-MM1; Leica Biosystems, Concord, Canada). Globo H immunohistochemical (IHC) analysis was performed on FFPE human and rat ICC tissues as described previously.[20] Details of IHC methods were described in the Supporting Information.

MATRIX-ASSISTED LASER DESORPTION IONIZATION–TIME-OF-FLIGHT ANALYSIS OF PERMETHYLATED GSLs

GSLs were extracted from human and rat ICC tissues as previously described.[21] Briefly, frozen tissue (approximately 25 mg) was homogenized and extracted with a mixture of methanol and chloroform. After centrifugation, the supernatant was collected, and the pellet was extracted three more times as described above. The pooled supernatants from each extraction were further separated into neutral and acidic GSLs by anion-exchange chromatography. Permethylated GSLs were mixed with matrix 2,5-dihydroxybenzoic acid (Sigma-Aldrich, Co., St. Louis, MO, USA) and acquired the mass spectrum profile by matrix-assisted laser desorption ionization-time of flight (MALDI-TOF; SCIEX 5800 TOF/TOF, Framingham, MA) with positive-ion mode and accumulated 4,000 laser shots with a random sampling mode.[22]

QUANTITATIVE REVERSE-TRANSCRIPTION REAL-TIME POLYMERASE CHAIN REACTION FOR DETECTION OF NATURAL KILLER CELL MARKERS

RNA was extracted from rat tumor tissues by homogenizing tissue samples in Tri-Reagent (Sigma-Aldrich, St. Louis, MO), in accordance with the manufacturer's protocol, and purified RNA (1 μg) was reverse-transcribed to complementary DNA (cDNA) using the High Capacity cDNA Reverse Transcription Kit (Applied Biosystems, Waltham, MA). Primer pairs for genes associated with natural killer (NK) cells were designed as described by Renaud et al.[23] and are listed in Supporting Table S1. Ten nanograms of cDNA template were added to each quantitative real-time polymerase chain reaction (PCR) reaction containing the Fast SYBR Green Master Mix (Applied Biosystems). Fluorescent signals were analyzed by Applied Biosystems 7500 Software v2.0.6, and relative messenger RNA expression was calculated using the ΔΔCt method.

MULTIPLEX IMMUNOFLUORESCENCE STAINING

Rat tumor specimens were assessed with multiplex IHC analysis, which provided simultaneous detection and quantitation of CD45 (leukocyte marker), CD56, CD161 (NK cell marker), and PAN-CK (tumor cell marker). Detailed methods are described in the Supporting Information.

STATISTICAL ANALYSIS

Data are presented as mean ± SD, count, and percentages. Survival curves were plotted by the Kaplan–Meier method, with the log-rank test applied for comparison, and the Cox proportional-hazards regression model was used to identify independent prognostic factors. Statistical analyses were performed with Prism 5.0 (GraphPad Software, La Jolla, CA) and SPSS (SPSS Inc., Chicago, IL) software.

Results

EXPRESSION OF GLOBO H IN ICC TISSUES

Mining of the data set for human ICC from the TIGER-LC revealed significantly higher expression of two genes involved in the biosynthesis of Globo H, beta-1,3-galactosyltransferase 5 (*B3GALT5*) and fucosyltransferase 2 (*FUT2*), in ICC tumor than the nontumor part by 3 fold and 8 fold, respectively (Fig. 1A). Analysis of the Cancer Genome Atlas data also indicated higher expression of B3GALT5 (15.5 fold), FUT1 (3.1 fold), and FUT2 (15.6 fold) in ICC tumor than in normal tissue (Supporting Fig. S1). This finding prompted us to examine the expression of Globo H on ICC specimens by IHC staining with monoclonal antibody against Globo H. As reported in our previous study, Globo H was not detected in the

normal liver by IHC or mass spectrometric analyses.[20] Representative positive and negative IHC stainings from ICC specimens are shown in Fig. 1B. In general, the staining patterns of Globo H were heterogeneous. In most cases, Globo H–positive cells were observed in clusters within the tumor, but occasionally dispersed Globo H–positive cells were also noted. Most of the Globo H–positive cells displayed membranous

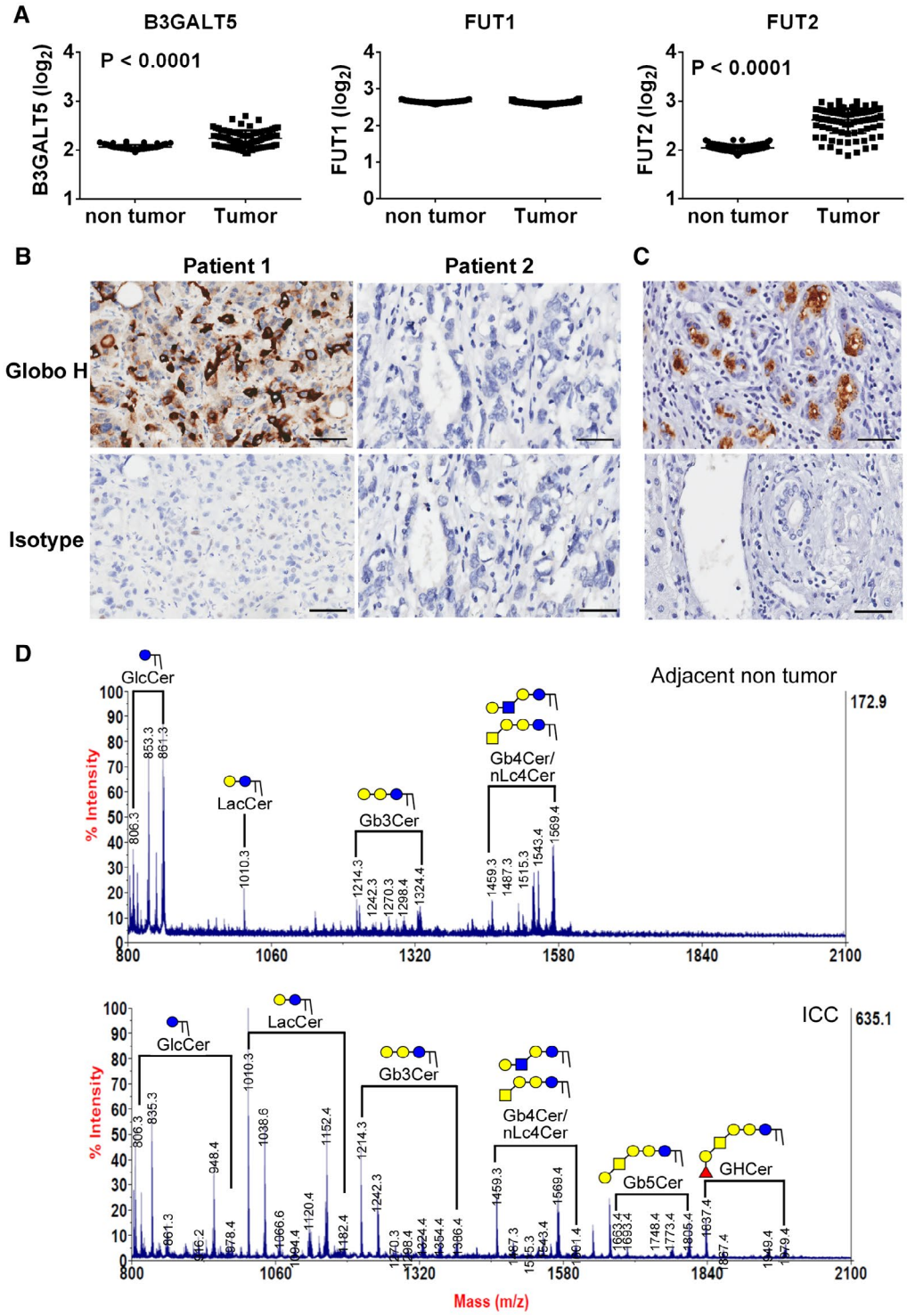

FIG. 1. Expression of Globo H and its biosynthetic enzymes in human cholangiocarcinoma. (A) RNA expression levels (log2) of *B3GALT5*, *FUT1*, and *FUT2* in ICC tumors were analyzed from the Human Transcriptome Array data sets GSE76311, which were obtained from TIGER-LC patients with ICC. The data are expressed as the mean ± SEM. (B) Expression of Globo H in formalin-fixed, paraffin-embedded ICC tissue sections was determined by IHC staining with mAbVK9. The representative positive (left panel) and negative (right panel) stainings for Globo H and their isotype controls from 2 patients with ICC were shown. Scale bars indicate 60 μm (original magnification ×40). (C) Expression of Globo H in a representative pair of ICC tumor part (upper panel) and adjacent nontumor part containing normal bile duct (lower panel) as determined by IHC staining with mAbVK9. (D) MALDI-TOF mass spectra of permethylated GSLs derived from a Globo H–positive human ICC tumor and adjacent nontumor tissue. Signals of Fuc1Hex4HexNAc1Cer (Globo H) and Hex4HexNAc1Cer (SSEA-3) were found in the neutral fraction of GSL extract. These GSLs carried both C16:0 and C24:0/C24:1 ceramides (at 112/110 mass units higher than those with C16:0).

and/or patchy cytoplasmic staining, whereas nuclear staining was rarely seen. Moreover, Globo H was not expressed in the adjacent normal liver tissue or bile duct (Fig. 1C). In light of the reported cross-reactivities of antiglycan antibodies observed in glycan array assays,[24] we confirmed the presence of Globo H by MALDI-TOF mass spectrometric analysis of GSLs extracted from two tumor tissues that stained positively for Globo H on IHC but absent in the adjacent noncancerous tissues (Fig. 1D, upper panel). On the basis of the mass-to-charge ratio (m/z) values of major molecular ion signals and the usual ranges of common permutations of sphingosine and fatty acyl along with the characteristics of GSLs, the signals of FucHex4HexNAc1Cer (m/z = 1,837/1,950) and Hex4HexNAc1Cer (m/z = 1,663/1,776) that represented Globo H and SSEA-3, respectively, with chain length of ceramide from C16 to C24 were found in the neutral fraction (Fig. 1D, lower panel).

GLOBO H EXPRESSION CORRELATES WITH POOR CLINICAL OUTCOME

Using IHC staining, Globo H expression with H-score ≧ 1 was detected in 63 of 155 (41%) of ICC tumor specimens. The possible association of Globo H expression with clinical pathological parameters in patients with ICC was analyzed. As given in Table 1, Globo H expression levels were significantly correlated with carbohydrate antigen 19-9 (P = 0.01), tumor number (P = 0.002), vascular invasion (P = 0.001), relapse (P < 0.001), and death (P < 0.001), indicating that Globo H expression is associated with aggressive tumor behaviors.

We further investigated whether positive expression of Globo H was a significant predictor for recurrence of ICC. Kaplan-Meier analysis revealed that relapse-free survival (RFS) in patients with positive expression of Globo H (median: 7.33 months, 95% confidence interval [CI]: 3.6-11.1 months), was significantly shorter than those with low expression of Globo H (median: 10.9 months, 95% CI: 7.9-13.9 months; P = 0.0003) (Fig. 2A). Kaplan-Meier analyses of OS showed that patients with positive expression of Globo H (median: 19.8 months, 95% CI: 17.9-21.7 months) had significantly poorer OS than those with low expression (median: 25.9 months, 95% CI: 14.1-37.6 months; P = 0.002) (Fig. 2B). More importantly, patients with stages I and II Globo H^+ ICC had significantly inferior RFS than the Globo H^- group (P = 0.009) at 1 year (44.7% vs. 63.0%), 3 years (11.2% vs. 36.9%), and 5 years (3.7% vs. 30.2%) (Fig. 2C). These patients also had significantly shorter OS than the Globo H^- group (P = 0.007) at 1 year (75% vs. 78.9%), 3 years (32.1% vs. 51.4%), and 5 years (17.9 vs. 40.8%) (Fig. 2D).

GLOBO H EXPRESSION IS AN INDEPENDENT RISK FACTOR FOR ICC

To evaluate the potential prognostic value of Globo H expression in ICC, univariate Cox proportional hazard regression analyses were conducted. As shown in Fig. 3A, RFS correlated with tumor size greater than 5 cm (hazard ratio [HR]: 2.29, 95% CI: 1.60-3.28; P < 0.001), multiple tumors (HR: 1.64, 95% CI: 1.07-2.51; P = 0.02), presence of vascular invasion (HR: 1.55, 95% CI: 1.08-2.22; P = 0.02), and presence of lymph node metastasis (HR: 1.98, 95% CI: 1.36-2.89; P < 0.001), consistent with the known adverse effects of these parameters. Importantly, positive expression of Globo H is associated with increased risk of tumor recurrence in patients with ICC (HR: 1.89, 95% CI: 1.33-2.70; P < 0.001). Furthermore, OS correlated

TABLE 1. ASSOCIATION OF GLOBO H EXPRESSION WITH CLINICAL-PATHOLOGICAL PARAMETERS IN 155 PATIENTS WITH ICC

		Globo H Expression		
Characteristics	n (%)	Negative (n = 92)	Positive (n = 63)	*P* Value
Age (mean [range]), years	60.5 (29-90)	60.7 (35-90)	60.2 (29-79)	0.79
Platelets, 10^9/L	231.7 (52-557)	233.5 (94-557)	229.3 (52-556)	0.80
Albumin, g/dL	3.7 (1.9-4.8)	3.6 (1.9-4.7)	3.8 (2.5-4.8)	0.08
Total bilirubin, mg/dL	1.4 (0.2-6.6)	1.19 (0.3-6.6)	1.0 (0.2-6.1)	0.11
AFP, ng/mL	22.8 (1-567)	27.2 (1-567)	16.9 (1.8-336)	0.95
CA19-9, U/mL	1,478.6 (0.6-10000)	748.6 (0.6-10,s000)	2,438.6 (2-10,000)	**0.01**
CEA, ng/mL	27.9 (0.5-593)	16.6(0.5-209.7)	43.1 (0.5-593)	0.06
Sex				
Male	73 (47.1%)	47	35	0.63
Female	82 (52.9%)	45	28	
Grade*				
I-II	90 (59.2%)	50	40	0.32
III	62 (40.8%)	40	22	
Stage				
I-II	81 (52.3%)	53	28	0.14
III	74 (47.7%)	39	35	
Tumor size				
≤ 5 cm	71 (45.8%)	48	23	0.07
> 5 cm	84 (54.2%)	44	40	
Tumor number				
Single	125 (80.6%)	82	43	**0.002**
multiple	30(19.4%)	10	20	
Vascular invasion				
No	99 (63.9%)	69	30	**0.001**
Yes	56 (36.1%)	23	33	
Encapsulation†				
Incomplete	127 (86.9%)	73	54	0.46
Complete	19 (13.1%)	13	6	
Lymph node metastasis				
No	110 (70.9%)	68	42	0.37
Yes	45 (29.1%)	24	21	
HBV infection‡				
No	78 (64.5%)	48	30	0.57
Yes	43 (35.5%)	24	19	
HCV infection§				
No	99 (81.8%)	55	44	0.09
Yes	22 (18.2%)	17	5	
Relapse (median ± SD and range) (months)	8.6 ± 40.4 (0.23-226)			
No	25 (16.1%)	24	1	**<0.001**
Yes	130 (83.9%)	68	62	
Death (median ± SD and range) (months)	19.2 ± 44.9 (0.23-226)			
No	27 (17.4%)	26	1	**<0.001**
Yes	128 (82.6%)	66	62	

#Statistically significant values are displayed in boldface.
*Data not available in 3 patients.
†Data not available in 9 patients.
‡Data not available in 34 patients.
§Data not available in 34 patients.
Abbreviations: AFP, alpha-fetoprotein; CA19-9, carbohydrate antigen 19-9; CEA, carcinoembryonic antigen; HBsAg, hepatitis B surface antigen; HBV, hepatitis B virus; HCV, hepatitis C virus.

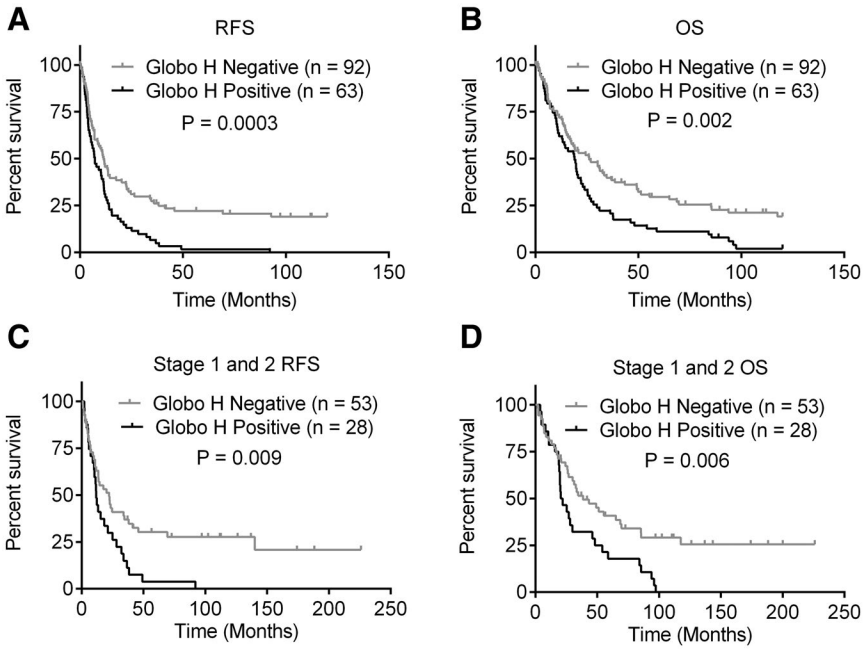

FIG. 2. Globo H expression correlates with shorter survival of patients with ICC. Kaplan-Meier survival analyses of RFS (A,C) and OS (B,D) of all patients with ICC (A,B) and early-stage (stage 1 and stage 2) patients (C,D) in relation to positive (H-score ≧ 1) or negative (H-score < 1) Globo H expression. Tumors with either nuclear, cytoplasmic, or membranous staining were considered to be positive for Globo H.

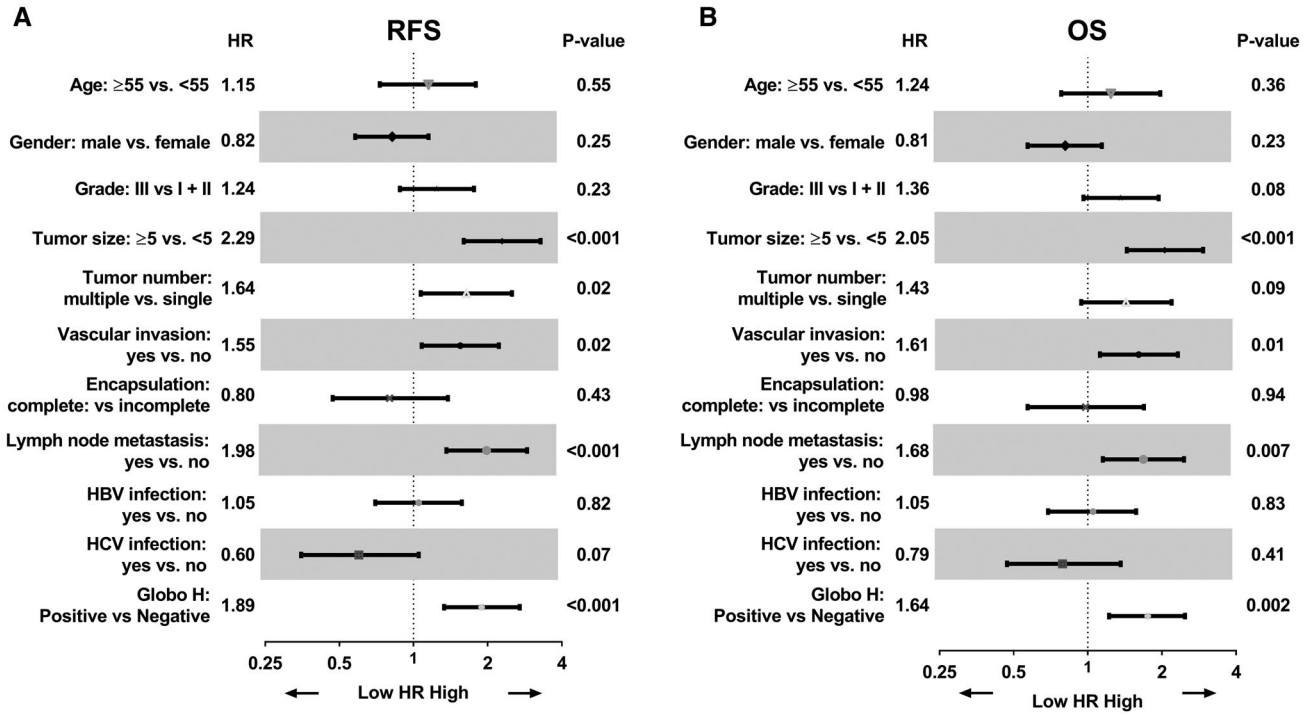

FIG. 3. Univariate analysis of positive Globo H expression as prognostic factors. Forest plot of univariate analysis. Factors associated with ICC were tested by univariate Cox analysis of for relapse RFS (A) and OS (B). Abbreviations: HBV, hepatitis B virus; HCV, hepatitis C virus.

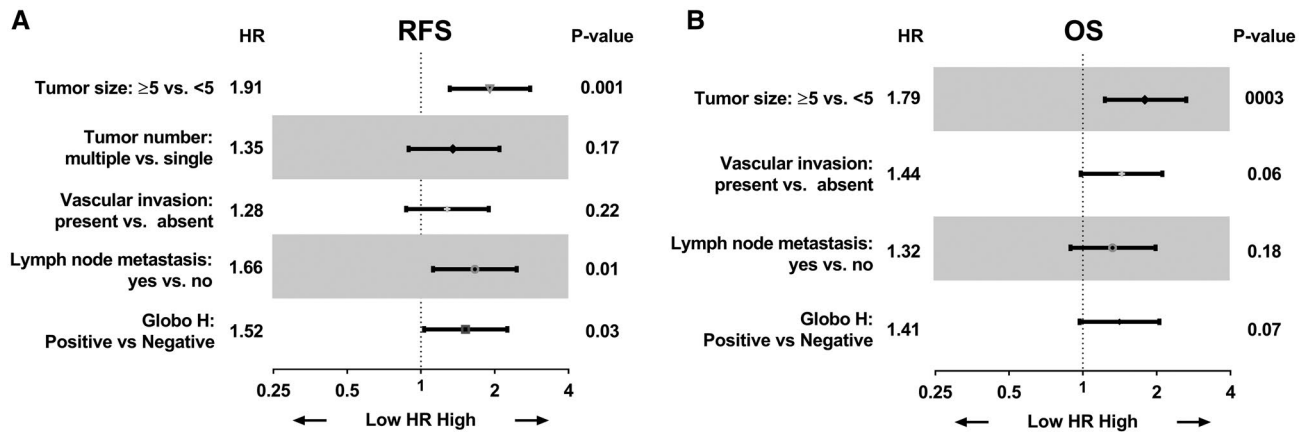

FIG. 4. Multivariate analysis of positive Globo H expression as prognostic factors. Forest plot of multivariate analysis. Factors associated with ICC were tested by multivariate Cox analysis of for relapse RFS (A) and OS (B).

with tumor size greater than 5 cm (HR: 2.05, 95% CI: 1.44-2.94; $P < 0.001$), presence of vascular invasion (HR: 1.61, 95% CI: 1.12-2.32; $P = 0.01$), and presence of lymph node metastasis (HR: 1.68, 95% CI: 1.15-2.46; $P = 0.007$), in line with the known prognostic impacts of these parameters. Additionally, OS of patients with ICC was significantly associated with positive expression of Globo H (HR: 1.75, 95% CI: 1.22-2.48; $P = 0.002$) (Fig. 3B). Next, we selected those important covariates that showed statistical significance in the univariate analysis for multivariable Cox regression analysis in a stepwise manner to identify the independent variables associated with poor RFS and OS. Our data indicated that tumor ≥ 5 cm was an independent risk factor for RFS and OS. Presence of lymph node metastasis was an independent risk factor for RFS. Notably, Globo H expression was an independent risk factor for recurrence (HR: 1.52, 95% CI: 1.03-2.25; $P = 0.03$) (Fig. 4A), although it did not reach statistical significance as an independent risk factor for OS (HR: 1.41, 95% CI: 0.97-2.05; $P = 0.07$) (Fig. 4B). These findings identified Globo H expression as an independent predictor for RFS in patients with ICC, implying that Globo H may play a critical role for cancer progression.

EXPRESSION OF GLOBO H IN TAA-INDUCED ICC TISSUES

Chronic administration of TAA can recapitulate the multistage progression of ICC in rat.[17] We performed Globo H IHC assay on tissues obtained from different stages of progression of ICC in rat. As shown in Fig. 5A, at 5 weeks following the administration of TAA, no discernible tumors were noted, and Globo H expression was not detected in normal appearing cholangioles. By the eighth week, multifocal bile ductular proliferation with demonstrable atypia (biliary dysplasia) with rare Globo H expression was observed. From the 15th to 21st week, the expression of Globo H was observed in 100% of atypical cholangiolar proliferation and invasive ICC tissues of livers. These findings imply that Globo H is associated with tumorigenesis of TAA-induced rat ICC. We also confirmed the presence of these glycans by mass spectrometric analysis of GSLs extracted from the rat tumor tissues that stained positively for Globo H on IHC. As analyzed by MALDI-TOF mass spectrometry, the signals of FucHex4HexNAc1Cer (m/z = 1,867/1,979) and Hex4HexNAc1Cer (m/z = 1,663/1,775), which represented Globo H and SSEA-3, respectively, were found in the neutral fraction of the GSL extraction (Fig. 5B).

GLOBO H ANTIBODY DISPLAYS ANTITUMOR EFFICACY AGAINST TAA-INDUCED ICC IN RAT

Anti-Globo H antibodies elicited by Globo-H vaccine in cancer patients have been shown to induce complement-dependent cytotoxicity (CDC) and antibody-dependent cellular cytotoxicity (ADCC).[25,26]

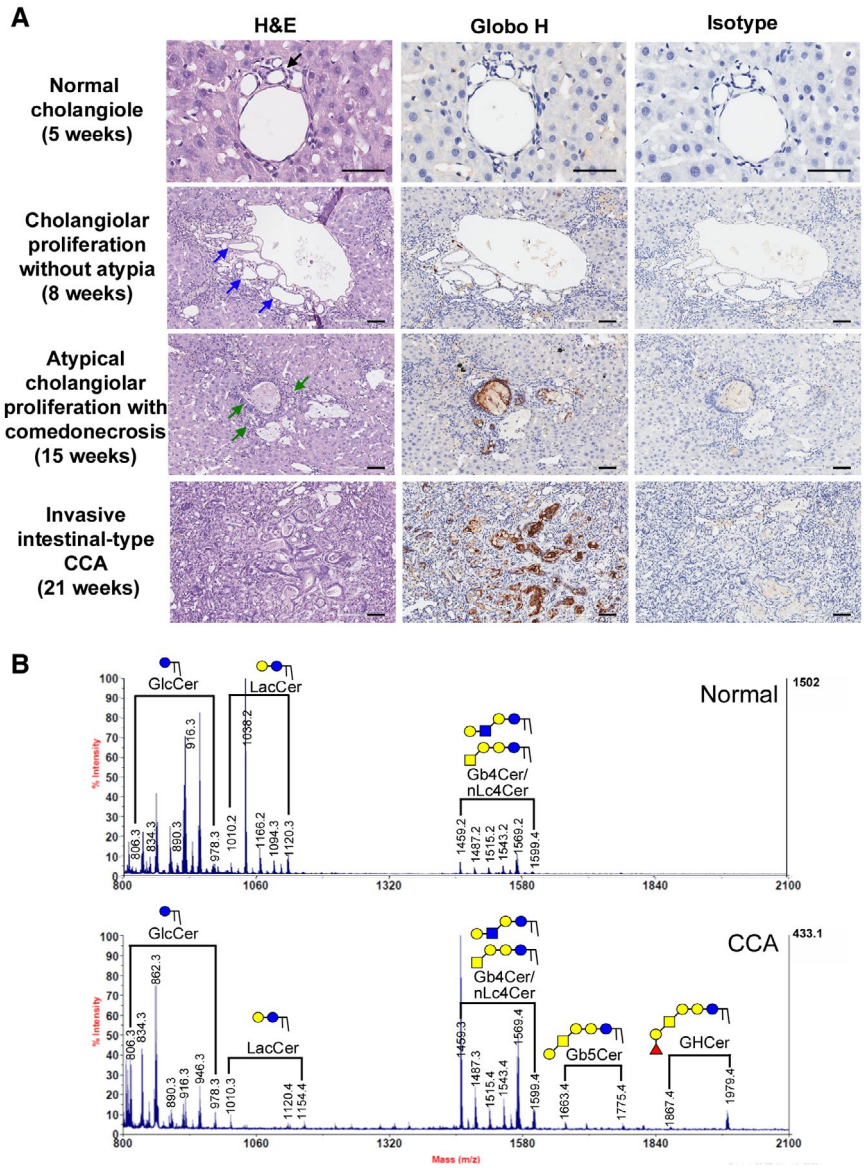

FIG. 5. Globo H expression in multistep progression model of rat ICC. (A) Globo H expression in rat liver after TAA treatment for increasing duration: normal cholangiole at 5 weeks, cholangiolar proliferation without atypia at 8 weeks, atypical cholangiolar proliferation with comedonecrosis at 15 weeks, and invasive intestinal-type ICC with intense stromal desmoplasia at 21 weeks. Scale bars indicate 60 μm (original magnification ×40) (black arrow indicates normal cholangiole; indigo arrows indicate bile duct proliferations; and green arrows indicate small atypical bile ductular proliferations). (B) MALDI-TOF MS spectra of permethylated GSLs derived from a Globo H–positive rat ICC tumor tissue. Signals of Fuc1Hex4HexNAc1Cer (Globo H) and Hex4HexNAc1Cer (SSEA-3) were found in the neutral fraction of GSLs from rat ICC tumor tissue. These GSLs carried both C16:0 and C24:0/C24:1 ceramides (at 112/110 mass units higher than those with C16:0). Abbreviation: H&E, hematoxylin and eosin.

We have recently reported that mAbVK9 can mediate CDC.[27] As shown in Supporting Fig. S2, mAbVK9 induced significant ADCC of GHCer-pretreated HuCCT1 cells with a mean percent lysis of 42.45% ± 5.1%, as compared with the isotype control of 9.79% ± 3.4% at the E:T ratio of 12.5:1 ($P < 0.05$). In SSP25 cells pretreated with GHCer, mAbVK9 induced 56.6% ± 20.8% lysis as compared with 9.48% ± 4.49% by isotype antibody ($P < 0.05$). These data indicated that mAbVK9 could mediate ADCC against Globo H–expressing HuCCT1 and SSP25 ICC cell lines. We evaluated the antitumor efficacy of mAbVK9 in

TAA-induced ICC in rats by ^{18}F-FDG-PET imaging in the cross-sectional planes as transverse, sagittal, and coronal views. At 24 weeks of TAA exposure, more than one FDG-avid tumors were detected in the liver of all rats, as demonstrated in the coronal view of the animal PET-CT (Fig. 6A). The mean standardized uptake value (SUV) of the normal and tumor liver tissues was calculated, and the respective tumor-to-liver (T/L) radioactivity ratios were determined. Rats were randomly assigned to two groups to receive intravenous treatment with anti-Globo H mAbVK9 (n = 5) or PBS as a control (n = 4) every other week for 8 weeks, while continued on TAA treatment. The T/L ratios of SUV were assessed at weeks 28 and 32. The fold changes of the T/L ratios at week 32 to the baseline at week 24 for each rat in the two groups are presented in Fig. 6B. There was a significant reduction in the fold change of T/L ratio of the SUV in the mAbVK9-treated group as compared with the control group (median of control vs. mAbVK9 treated group: 1.36 vs. 0.69, $P = 0.01$) (Fig. 6B). On the other hand, there was no significant difference in the body weight between the mAbVK9-treated and control group (Supporting Fig. S3). At the end of therapy, ICC tumors were harvested and examined for the proliferation of tumor cells and infiltration of NK cells. As shown in Fig. 6C, a dramatic decrease in the proliferation of tumor cells as measured by Ki67 staining was observed in the mAbVK9 treatment group ($P = 0.017$). Along this line, staining intensity for tumor marker, PanCK, also decreased significantly in the mAbVK9 treatment group, as compared with the control group (Supporting Fig. S4). Using multiplex IHC/immunofluorescence with anti-CD56/CD45 or anti-CD161/CD56 to assess NK cells in the tumor microenvironment, we observed that the median density of CD56+/CD45+ cells was significantly greater in the mAbVK9 treatment group (68/mm^2 [range 52-72]) than the control group (12.46/mm^2 [range 11-20]) ($P = 0.015$) (Fig. 6D). Similarly, the median density of CD56+/CD161+ cells was also significantly greater in the mAbVK9 treatment group (51.6/mm^2 [range 43-65] than the control group (11/mm^2 [range 8-21]) ($P = 0.02$) (Supporting Fig. S5). This is consistent with the increased expression of NK markers as assessed by quantitative real-time PCR. The transcripts analyzed included Prf1 (encodes perforin), Ifng (encodes interferon-gamma), and a variety of NK-specific receptors, such as Ly49s5/i5 and Ly49s3/s4/i3/i4 (which encode Ly49/killer cell lectin-like A receptors), killer cell lectin-like receptor (Klr) B1, Klrb1a, and Klrb1b (which encode killer cell lectin-like B receptors), and Ncr1 (natural cytotoxicity triggering receptor). Compared with the control group, expression of these genes associated with NK cells was significantly increased in the group treated with mAbVK9 (Fig. 6E). Expression of other non-NK-specific transcripts (interleukin [*Il*]-18 and lysosomal-associated membrane protein 1) were not affected. Collectively, these data indicated that NK cells were enriched in the tumor microenvironment of TAA-induced ICC following mAbVK9 treatment, contributing to the antitumor activity of Globo H antibody in the rat ICC model.

Discussion

Although multiple studies have identified Globo H as a tumor-associated carbohydrate antigen that is overexpressed in most epithelial cancers, including HCC, its expression in ICC has yet to be determined. A study of lung cancer shows an association of positive Globo H expression with epidermal growth factor receptor mutation and programmed death ligand 1 (PD-L1) expression in lung adenocarcinoma and with PI3KCA overexpression in squamous cell carcinoma.[28] Another study reports an association of Globo H expression with American Thyroid Association risk of recurrence of papillary thyroid cancer.[29] However, the prognostic value of Globo H in cancer has yet to be investigated. Here, we showed that the Globo H is positively expressed in 41% of ICC clinical samples based on IHC staining, and confirmed by MALDI-TOF mass spectrometry. Moreover, Cox regression analysis demonstrated that patients with Globo H–positive tumors experienced significantly worse OS and RFS than those with Globo H–low tumors, while multivariate analysis revealed Globo H expression to be an independent risk factor for ICC recurrence, suggesting that Globo H is a prognostic marker for ICC.

Our result showed that Globo H–positive staining was occasionally noted in normal proliferative cholangiocytes. It has been reported that the biosynthetic enzymes for Globo H biosynthesis, FUT1 and FUT2, are up-regulated by pro-inflammatory cytokines such as IL-1β.[30] IL-1β is released by hepatocytes through inflammasome activation. In

experimental models of nonalcoholic fatty liver disease mice and TAA rat model, increased IL-1β secretion by hepatocytes has been shown to drive liver fibrosis.[31,32] These considerations might explain the occasional detection of Globo H in the proliferative cholangiocytes.

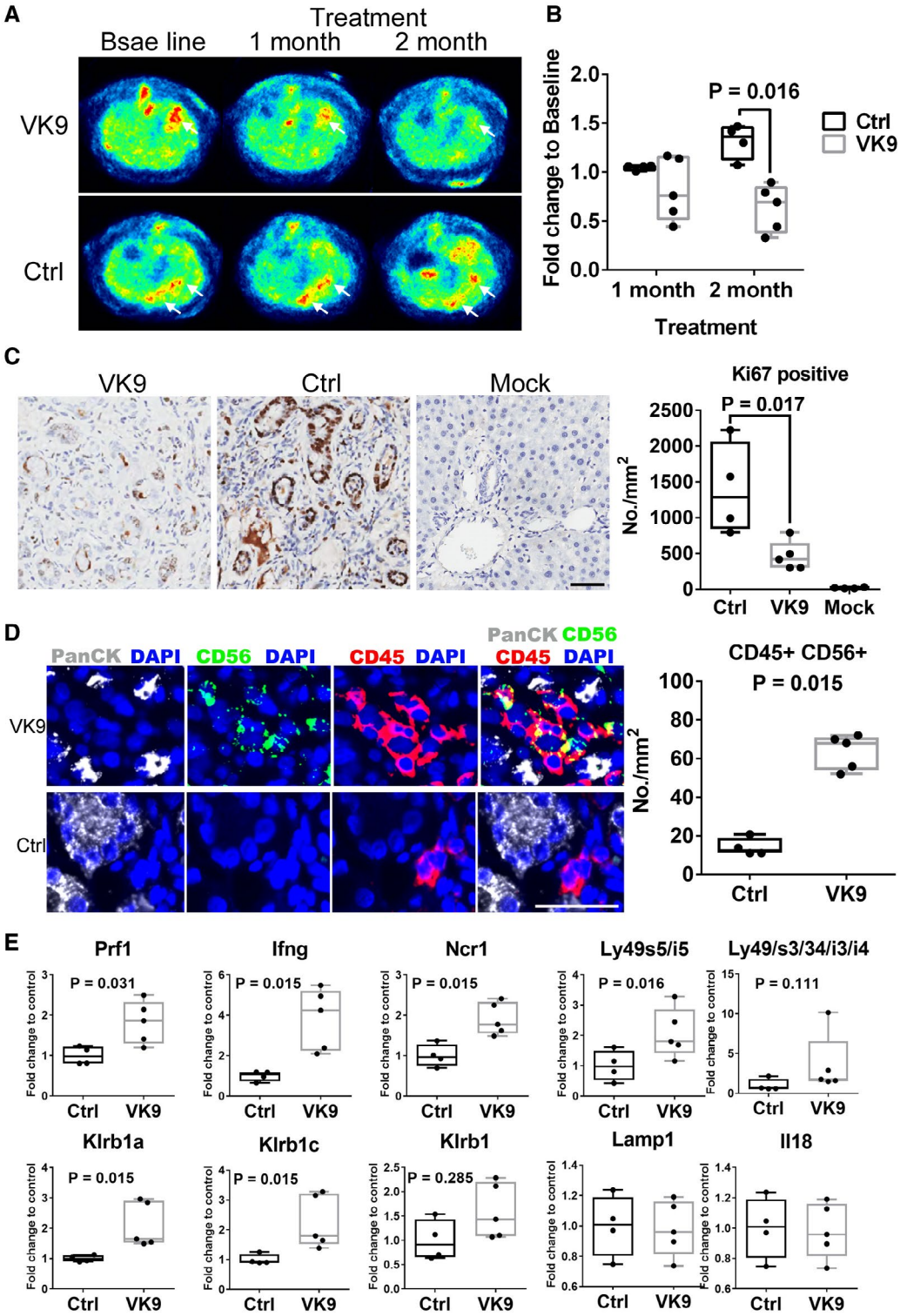

FIG. 6. Anti-Globo H antibody suppresses tumor growth in rat ICC model. (A) Following the administration of TAA for 24 weeks, rats exhibiting ^{18}F-FDG-PET-detectable tumors were treated intravenously with 300 μg anti-Globo H antibody, mAbVK9 (n = 5), or PBS (n = 4) every week for 8 weeks. Arrowheads indicate tumor sites. (B) Alterations of SUV at 1 and 2 month following treatment with mAbVK9. The 18 F-FDG uptake by tumors was quantified using SUV mean, and the fold change was calculated by normalizing ^{18}F-FDG uptake after treatment to baseline for each animal. (C) IHC staining for Ki67 in rat ICC tissue of the mAbVK9-treated group, control group, and vehicle-treated group. At the end of treatment, rats were sacrificed and liver was excised for IHC studies. Randomly selected areas from each tumor were analyzed. The number of Ki67-positive cells per square millimeter as compared between the mAbVK9-treated group and control group using StrataQuest. Scale bars indicate 60 μm (original magnification ×40). (D) Left panels are representative photomicrographs of multiplex panel (PanCK, white; CD56, green; CD45, red; and 4′,6-diamidino-2-phenylindole) from rats treated with mAbVK9 or PBS control. Right panel shows the number of CD45-positive and CD56-positive cells per square millimeter in the mAbVK9-treated group and control group using Metamorph. Scale bars indicate 60 μm (original magnification ×40; Student *t* test). (E) Quantitative real-time PCR analysis of the indicated NK cell markers in the mAbVk9-treated group and control group. Lysosomal-associated membrane protein 1 (Lamp1) and IL-18 represented non-NK cell markers. Graphs represent means ± SEM. Abbreviations: Ctrl, control; DAPI, 4′,6-diamidino-2-phenylindole; Ifng, interferon-gamma; Klr, killer cell lectin-like receptor; Ncr1, natural cytotoxicity triggering receptor; Prf1, perforin.

Previously, our group had reported that GHCer plays a crucial role in tumor progression by enhancing angiogenesis and promoting immunosuppression. Its angiogenic activity can be attributed to the uptake of GHCer shed from tumor cells by endothelial cells, with the subsequent binding of GHCer to translin-associated factor X, disrupting its interaction with phospholipase Cβ1, allowing the latter to induce calcium influx to drive endothelial cell proliferation, migration, and tube formation.[15] In a separate study, we have elucidated the mechanism by which GHCer acts as an immune checkpoint to facilitate cancer cell escape from immune surveillance, through suppression of Notch1 signaling.[16] These properties of GHCer provide a favorable microenvironment for tumor growth, which may explain the unfavorable outcome of patients with ICC with Globo H overexpression.

In the present study, the TAA-induced rat CCA model, which recapitulates the multistage progression of human cholangiocarcinoma, provides a valuable opportunity to demonstrate the gradual emergence of Globo H on ICC tissues over time *in vivo*. Although there has been increasing interest in the development of Globo H–based cancer immunotherapy due to the promising results from early clinical trials in breast cancer and prostate cancer,[13,25] preclinical testings have been limited to animal models of human cancers in immunodeficient mice. There is an urgent need for Globo H–expressing tumors in immunocompetent animal models. This carcinogen-induced ICC model in immunocompetent rats provides a valuable platform to fill the void for preclinical studies of Globo H–targeted therapeutics. Furthermore, Globo H was detected in regions of atypical cholangiolar proliferation at week 15 of TAA administration. Its detection in precursor lesions of ICC and tumor tissues, coupled with the reports that Globo H is shed from tumor cells into exosomes[15] and Globo H expression is highly associated with cancer stem cell properties,[20,33] makes Globo H a potential tissue and serum biomarker for early diagnosis of ICC. Further investigations along this line in the future are warranted. If confirmed, it will have important clinical implications because only early-stage disease is amenable to potentially curative surgical extirpation.

Our *in vivo* study in rats with TAA-induced ICC demonstrated promising antitumor efficacy of monoclonal anti-Globo H antibody, VK9. In general, the therapeutic effects of antibodies against tumor-associated antigens are mediated by CDC and ADCC. Likewise, anti-Globo H antibodies elicited by Globo-H vaccine in cancer patients have been shown to induce CDC and ADCC in the phase 1 clinical trials.[25,26] We have recently reported that mAbVK9 can mediate CDC.[27] The finding from this study also indicates that VK9 could induce ADCC against the Globo H–expressing cancer cell line. Moreover, we observed increased NK cells and significant upregulation of several NK cell markers in the ICC tumor microenvironment of mAbVK9 treated rats. In addition to being a major player in ADCC, NK cells are known to display antitumor activity *per se*, as reflected by inhibition of tumor growth in nude mice bearing human ICC xenograft infusion of *ex vivo* expanded human NK cells.[34] Our findings of NK cell activation following mAbVK9 treatment suggests that both direct cytotoxicity and ADCC may underlie the mechanisms for its antitumor efficacy in our

study. Previously, we showed that GHCer was shed from tumor cells into the tumor microenvironment to act as an immune checkpoint and an angiogenic factor to facilitate tumor growth. Therefore, in addition to ADCC, antibody against Globo H may neutralize the released GHCer to block its immune checkpoint and angiogenic functions.[15,16] Although immune checkpoint inhibitors have been considered a major breakthrough for cancer immunotherapy, pembrolizumab and nivolumab as single agents showed limited efficacy in advanced biliary tract cancer (BTC).[35,36] The programmed cell death-1/PD-L1 blockade is approved for treatment of a variety of advanced cancers with microsatellite instability–high, deficient mismatch repair or high tumor mutation burden–high,[37] but these genetic alterations rarely occur in BTCs, including ICC.[4] Thus, clinical trials of combination of ICIs and chemotherapy in BTCs, dendritic cell–based vaccine, and chimeric antigen receptor T cell–based therapy are being pursued.[38-40] In this context, our findings of Globo H as a theranostic target for Globo H coupled with the promising antitumor activities of an antibody against Globo H may add an armamentarium for the immunotherapy of ICC.

Acknowledgment: The authors thank the Tissue Bank and Biobank of Linkou Chang Gung Memorial Hospital for providing the ICC samples and related clinical data for the study.

REFERENCES

1) Ramanan P, Cummins NW, Wilhelm MP, Heimbach JK, Dierkhising R, Kremers WK, et al. Epidemiology, risk factors, and outcomes of infections in patients undergoing liver transplantation for hilar cholangiocarcinoma. Clin Transplant 2017;31:e13023.
2) Khan SA, Tavolari S, Brandi G. Cholangiocarcinoma: epidemiology and risk factors. Liver Int 2019;39(Suppl. 1):19-31.
3) Mavros MN, Economopoulos KP, Alexiou VG, Pawlik TM. Treatment and prognosis for patients with intrahepatic cholangiocarcinoma: systematic review and meta-analysis. JAMA Surg 2014;149:565-574.
4) Wu CE, Pan YR, Yeh CN, Lunec J. Targeting P53 as a future strategy to overcome gemcitabine resistance in biliary tract cancers. Biomolecules 2020;10:1474.
5) Chiang NJ, Chen LT, Shan YS, Yeh CN, Chen MH. Development of possible next line of systemic therapies for gemcitabine-resistant biliary tract cancers: a perspective from clinical trials. Biomolecules 2021;11:97.
6) Goyal L, Shi L, Liu LY, Fece de la Cruz F, Lennerz JK, Raghavan S, et al. TAS-120 overcomes resistance to ATP-competitive FGFR inhibitors in patients with FGFR2 fusion-positive intrahepatic cholangiocarcinoma. Cancer Discov 2019;9:1064-1079.
7) Ross JS, Wang K, Gay L, Al-Rohil R, Rand JV, Jones DM, et al. New routes to targeted therapy of intrahepatic cholangiocarcinomas revealed by next-generation sequencing. Oncologist 2014;19:235-242.
8) Abou-Alfa GK, Macarulla T, Javle MM, Kelley RK, Lubner SJ, Adeva J, et al. Ivosidenib in IDH1-mutant, chemotherapy-refractory cholangiocarcinoma (ClarIDHy): a multicentre, randomised, double-blind, placebo-controlled, phase 3 study. Lancet Oncol 2020;21:796-807.
9) Yu AL, Gilman AL, Ozkaynak MF, Naranjo A, Diccianni MB, Gan J, et al. Long-term follow-up of a phase III study of ch14.18 (dinutuximab) + cytokine immunotherapy in children with high-risk neuroblastoma: COG study ANBL0032. Clin Cancer Res 2021;27:2179-2189.
10) Gu J, Sato Y, Kariya Y, Isaji T, Taniguchi N, Fukuda T. A mutual regulation between cell-cell adhesion and N-glycosylation: implication of the bisecting GlcNAc for biological functions. J Proteome Res 2009;8:431-435.
11) Matsuda A, Higashi M, Nakagawa T, Yokoyama S, Kuno A, Yonezawa S, et al. Assessment of tumor characteristics based on glycoform analysis of membrane-tethered MUC1. Lab Invest 2017;97:1262.
12) Talabnin K, Talabnin C, Ishihara M, Azadi P, Wongkham S, Sripa B. Differential expression of O-glycoprotein glycans in cholangiocarcinoma cell lines. Asian Pac J Cancer Prev 2016;17:691-695.
13) Huang C-S, Yu AL, Tseng L-M, Chow LWC, Hou M-F, Hurvitz SA, et al. Globo H-KLH vaccine adagloxad simolenin (OBI-822)/OBI-821 in patients with metastatic breast cancer: phase II randomized, placebo-controlled study. J Immunother Cancer 2020;8:e000342.
14) Zhang S, Cordon-Cardo C, Zhang HS, Reuter VE, Adluri S, Hamilton WB, et al. Selection of tumor antigens as targets for immune attack using immunohistochemistry: I. Focus on gangliosides. Int J Cancer 1997;73:42-49.
15) Cheng J-Y, Wang S-H, Lin J, Tsai Y-C, Yu J, Wu J-C, et al. Globo-H ceramide shed from cancer cells triggers translin-associated factor X-dependent angiogenesis. Cancer Res 2014;74:6856-6866.
16) Tsai YC, Huang JR, Cheng JY, Lin JJ, Hung JT, Wu YY, et al. A prevalent cancer associated glycan, globo H ceramide, induces immunosuppression by reducing notch1 signaling. J Cancer Sci Ther 2013;5:264-270.
17) Yeh CN, Maitra A, Lee KF, Jan YY, Chen MF. Thioacetamide-induced intestinal-type cholangiocarcinoma in rat: an animal model recapitulating the multi-stage progression of human cholangiocarcinoma. Carcinogenesis 2004;25:631-636.
18) Yeh C-N, Lin K-J, Hsiao I-T, Yen T-C, Chen T-W, Jan Y-Y, et al. Animal PET for thioacetamide-induced rat cholangiocarcinoma: a novel and reliable platform. Mol Imaging Biol 2008;10:209-216.
19) Chen M-H, Chiang K-C, Cheng C-T, Huang S-C, Chen Y-Y, Chen T-W, et al. Antitumor activity of the combination of an HSP90 inhibitor and a PI3K/mTOR dual inhibitor against cholangiocarcinoma. Oncotarget 2014;5:2372-2389.
20) Kuo H-H, Lin R-J, Hung J-T, Hsieh C-B, Hung T-H, Lo F-Y, et al. High expression FUT1 and B3GALT5 is an independent predictor of postoperative recurrence and survival in hepatocellular carcinoma. Sci Rep 2017;7:10750.
21) Ho MY, Yu AL, Yu J. Glycosphingolipid dynamics in human embryonic stem cell and cancer: their characterization and biomedical implications. Glycoconj J 2017;34:765-777.
22) Lin RJ, Kuo MW, Yang BC, Tsai HH, Chen K, Huang JR, et al. B3GALT5 knockout alters gycosphingolipid profile and facilitates transition to human naive pluripotency. Proc Natl Acad Sci U S A 2020;117:27435-27444.
23) Renaud SJ, Scott RL, Chakraborty D, Rumi MA, Soares MJ. Natural killer-cell deficiency alters placental development in rats. Biol Reprod 2017;96:145-158.

24) Wang C-C, Huang Y-L, Ren C-T, Lin C-W, Hung J-T, Yu J-C, et al. Glycan microarray of Globo H and related structures for quantitative analysis of breast cancer. Proc Natl Acad Sci U S A 2008;105:11661-11666.
25) Slovin SF, Ragupathi G, Adluri S, Ungers G, Terry K, Kim S, et al. Carbohydrate vaccines in cancer: immunogenicity of a fully synthetic globo H hexasaccharide conjugate in man. Proc Natl Acad Sci U S A 1999;96:5710-5715.
26) Gilewski T, Ragupathi G, Bhuta S, Williams LJ, Musselli C, Zhang X-F, et al. Immunization of metastatic breast cancer patients with a fully synthetic globo H conjugate: a phase I trial. Proc Natl Acad Sci U S A 2001;98:3270-3275.
27) Lin W-D, Fan T-C, Hung J-T, Yeo H-L, Wang S-H, Kuo C-W, et al. Sialylation of CD55 by ST3GAL1 facilitates immune evasion in cancer. Cancer Immunol Res 2021;9:113-122.
28) Yang CY, Lin MW, Chang YL, Wu CT. Globo H expression is associated with driver mutations and PD-L1 expressions in stage I non-small cell lung cancer. Cancer Biomark 2017;21:211-220.
29) Cheng SP, Yang PS, Chien MN, Chen MJ, Lee JJ, Liu CL. Aberrant expression of tumor-associated carbohydrate antigen Globo H in thyroid carcinoma. J Surg Oncol 2016;114:853-858.
30) Padro M, Mejias-Luque R, Cobler L, Garrido M, Perez-Garay M, Puig S, et al. Regulation of glycosyltransferases and Lewis antigens expression by IL-1beta and IL-6 in human gastric cancer cells. Glycoconj J 2011;28:99-110.
31) Salguero Palacios R, Roderfeld M, Hemmann S, Rath T, Atanasova S, Tschuschner A, et al. Activation of hepatic stellate cells is associated with cytokine expression in thioacetamide-induced hepatic fibrosis in mice. Lab Invest 2008;88:1192-1203.
32) Amanzada A, Moriconi F, Mansuroglu T, Cameron S, Ramadori G, Malik IA. Induction of chemokines and cytokines before neutrophils and macrophage recruitment in different regions of rat liver after TAA administration. Lab Invest 2014;94:235-247.
33) Chang W-W, Lee CH, Lee P, Lin J, Hsu C-W, Hung J-T, et al. Expression of Globo H and SSEA3 in breast cancer stem cells and the involvement of fucosyl transferases 1 and 2 in Globo H synthesis. Proc Natl Acad Sci U S A 2008;105:11667-11672.
34) Jung IH, Kim DH, Yoo DK, Baek SY, Jeong SH, Jung DE, et al. In Vivo study of natural killer (NK) cell cytotoxicity against cholangiocarcinoma in a nude mouse model. Vivo 2018;32:771-781.
35) Piha-Paul SA, Oh DY, Ueno M, Malka D, Chung HC, Nagrial A, et al. Efficacy and safety of pembrolizumab for the treatment of advanced biliary cancer: results from the KEYNOTE-158 and KEYNOTE-028 studies. Int J Cancer 2020;147:2190-2198.
36) Kim RD, Chung V, Alese OB, El-Rayes BF, Li D, Al-Toubah TE, et al. A phase 2 multi-institutional study of nivolumab for patients with advanced refractory biliary tract cancer. JAMA Oncol 2020;6:888-894.
37) Le DT, Durham JN, Smith KN, Wang H, Bartlett BR, Aulakh LK, et al. Mismatch repair deficiency predicts response of solid tumors to PD-1 blockade. Science 2017;357:409-413.
38) Jakubowski CD, Azad NS. Immune checkpoint inhibitor therapy in biliary tract cancer (cholangiocarcinoma). Chin Clin Oncol 2020;9:2.
39) Shimizu K, Kotera Y, Aruga A, Takeshita N, Takasaki K, Yamamoto M. Clinical utilization of postoperative dendritic cell vaccine plus activated T-cell transfer in patients with intrahepatic cholangiocarcinoma. J Hepatobiliary Pancreat Sci 2012;19:171-178.
40) Guo Y, Feng K, Liu Y, Wu Z, Dai H, Yang Q, et al. Phase I study of chimeric antigen receptor-modified T cells in patients with EGFR-positive advanced biliary tract cancers. Clin Cancer Res 2018;24:1277-1286.

Supporting Information

Additional Supporting Information may be found at onlinelibrary.wiley.com/doi/10.1002/hep4.1800/suppinfo.